Appendix 1. The statistics of raw data for sequencing transcriptome.

Sample	Read length (R1; R2)	Sequencing Reads quantity	Total length of sequencing read (Gb)
HCV	100;100	21,827,299	4.36
Blank	100;100	42,588,251	8.50

Appendix 2. Quality of pretreatment transcriptome data.

Sample	Raw data			Valid data			Valid Ratio (Reads)
	Reads	N_base	Length	Reads	N_base	Length	
Blank 1	42,588,251	14,276,600	101	26,253,644	0	25-101	61.65%
Blank 2	42,588,251	2,797,900	101	24,741,808	0	25-101	58.10%
HCV 1	21,827,299	6,680,000	101	17,317,956	0	25-101	79.34%
HCV 2	21,827,299	611,300	101	16,753,438	0	25-101	76.75%

Appendix 3. The Statistics of Gene Mapping for transcriptome data.

Sample	Clean Reads	Gene Mapped Reads	Gene Mapped Ratio	Gene Unique Reads	Gene Unique Ratio
HCV	34,071,394	20,068,969	58.90%	10,953,790	54.58%
Blank	52,507,288	31,012,192	59.06%	16,931,528	54.60%

Appendix 4. The mapped data of transcriptome.

Sample	Mapped Reads	Reads Perfact Match (%)	Reads 1 Mismatch	Reads 2 Mismatch	Reads Unique Count
HCV	20,068,969	15,075,202 (75.12%)	3,200,529 (15.95%)	1,793,238 (8.94%)	10,953,790 (54.58%)
Blank	31,012,192	23,607,123 (76.12%)	4,741,586 (15.29%)	2,663,483 (8.59%)	16,931,528 (54.60%)

Appendix 5. The data mapped genes of transcriptome.

Sample	Reads Multi Pos	Gene Num	Gene MAX Mapped Reads	Gene Average Mapped Reads
HCV	9,115,179 (45.42%)	29,573	390,597	678
Blank	14,080,664 (45.40%)	29,769	771,586	1,041

Appendix 6. Kolmogorov-Smirnov test for transcriptome data.

Sample	D value	*P* value
HCV	0.645	0.377
Blank	0.633	0.400

Appemdix 7. Kyoto Encyclopedia of Genes and Genomes (KEGG) analysis of upregulation metabolic pathways.

A

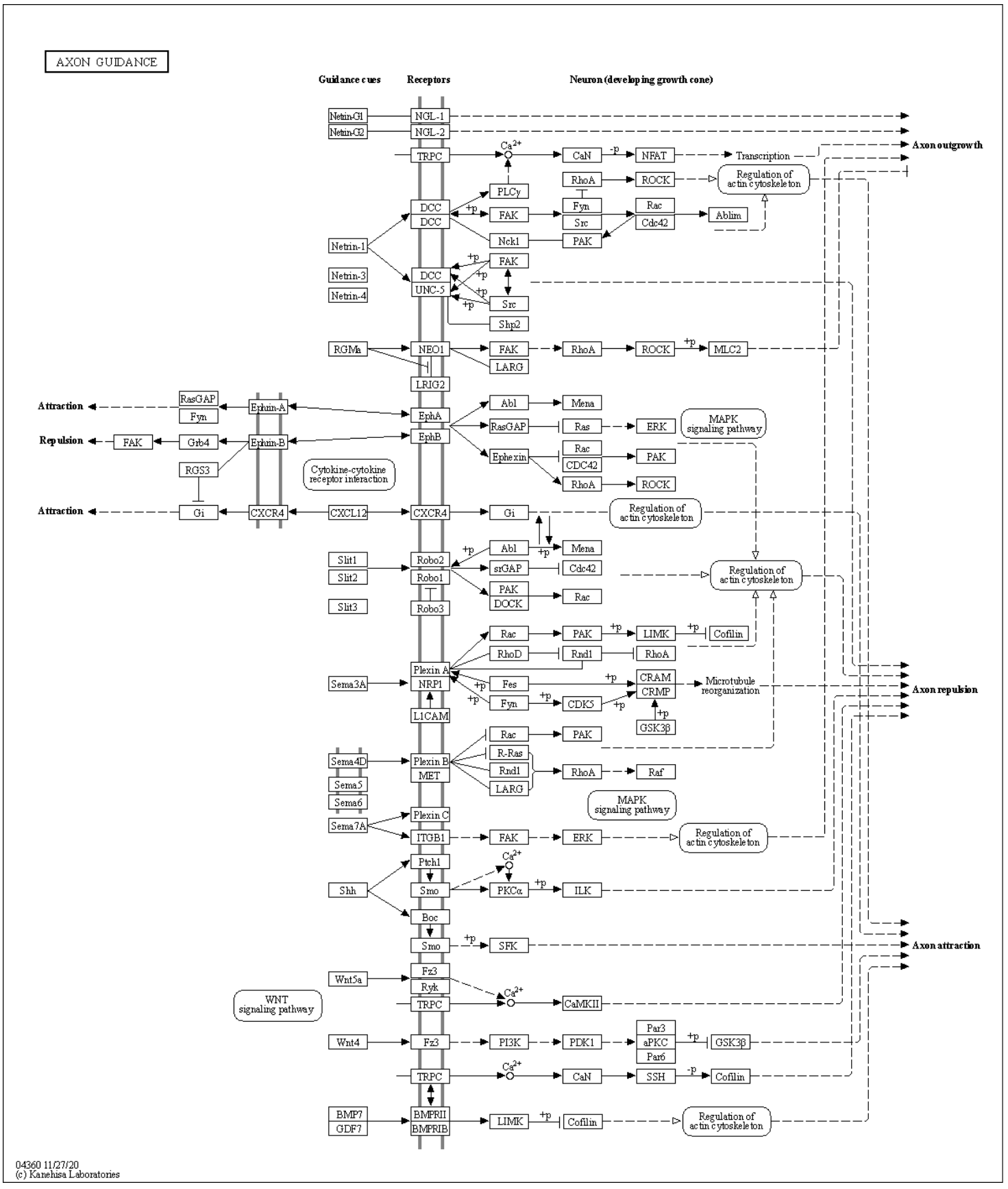

B

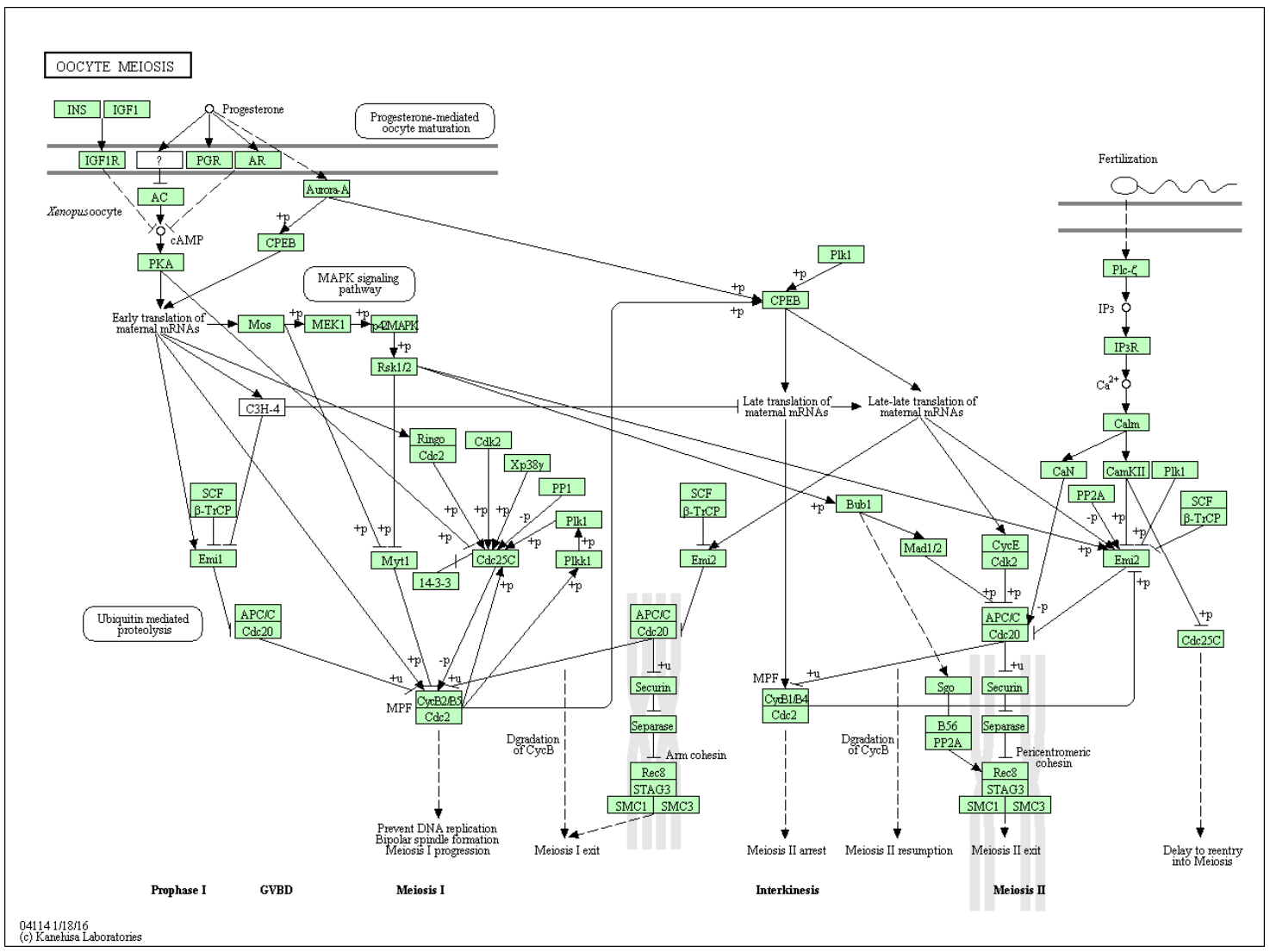
OOCYTE MEIOSIS
INS
IGF1
Progesterone
Progesterone-mediated oocyte maturation
IGF1R
?
PGR
AR
AC
Xenopus oocyte
cAMP
PKA
Aurora-A
CPEB
MAPK signaling pathway
Early translation of maternal mRNAs
Mos
MEK1
p42MAPK
Rsk1/2
C3H-4
Ringo
Cdc2
Cdk2
Xp38γ
PP1
Plk1
SCF
β-TrCP
Emi1
Myt1
Cdc25C
14-3-3
Ubiquitin mediated proteolysis
APC/C
Cdc20
MPF
CycB2/B5
Cdc2
Prevent DNA replication
Bipolar spindle formation
Meiosis I progression
Degradation of CycB
Securin
Separase
Arm cohesin
Rec8
STAG3
SMC1
SMC3
Meiosis I exit
Late translation of maternal mRNAs
Late-late translation of maternal mRNAs
Plk1
Bub1
Mad1/2
CycE
Cdk2
Emi2
Meiosis II arrest
CycB1/B4
Cdc2
Meiosis II resumption
Sgo
B56
PP2A
Pericentromeric cohesin
Meiosis II exit
Fertilization
Plc-ζ
IP3
IP3R
Ca2+
Calm
CaN
CamKII
Plk1
PP2A
Cdc25C
Delay to reentry into Meiosis
Prophase I
GVBD
Meiosis I
Interkinesis
Meiosis II
04114 1/18/16
(c) Kanehisa Laboratories

C

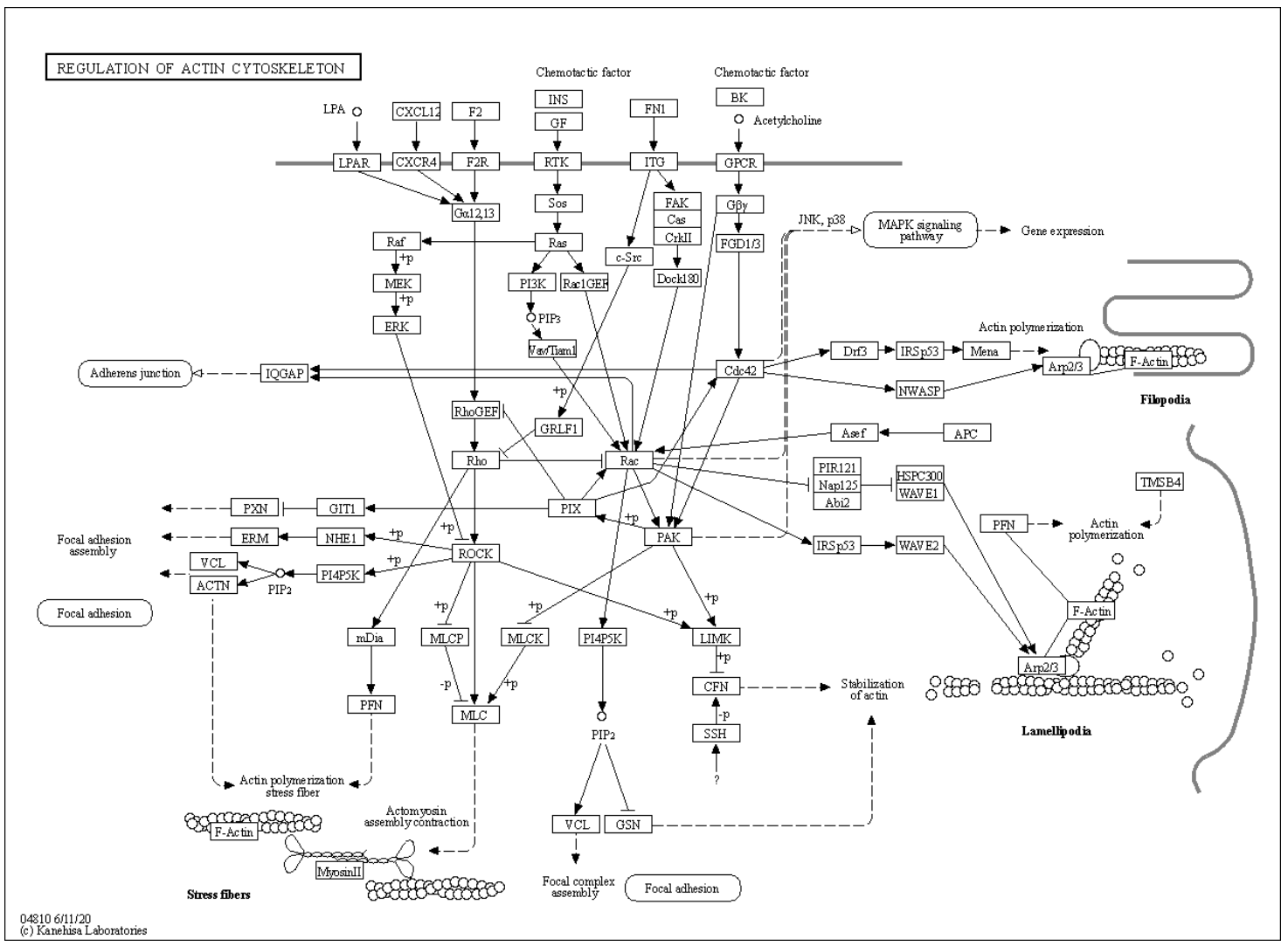
REGULATION OF ACTIN CYTOSKELETON
Chemotactic factor
Chemotactic factor
LPA
CXCL12
F2
INS
GF
FN1
BK
Acetylcholine
LPAR
CXCR4
F2R
RTK
ITG
GPCR
Gα12,13
Sos
FAK
Cas
CrkII
Gβγ
JNK, p38
MAPK signaling pathway
Gene expression
Raf
Ras
c-Src
FGD1/3
MEK
PI3K
Rac1GEF
Dock180
ERK
PIP3
Vav/Tiam1
Actin polymerization
Adherens junction
IQGAP
Cdc42
Drf3
IRSp53
Mena
Arp2/3
F-Actin
NWASP
Filopodia
RhoGEF
GRLF1
Asef
APC
Rho
Rac
PIR121
Nap125
Abi2
HSPC300
WAVE1
TMSB4
PXN
GIT1
PIX
PAK
PFN
Actin polymerization
Focal adhesion assembly
ERM
NHE1
ROCK
IRSp53
WAVE2
VCL
ACTN
PI4P5K
PIP2
Focal adhesion
F-Actin
mDia
MLCP
MLCK
PI4P5K
LIMK
Arp2/3
PFN
MLC
CFN
Stabilization of actin
Lamellipodia
PIP2
SSH
?
Actin polymerization stress fiber
Actomyosin assembly contraction
F-Actin
VCL
GSN
MyosinII
Stress fibers
Focal complex assembly
Focal adhesion
04810 6/11/20
(c) Kanehisa Laboratories

D

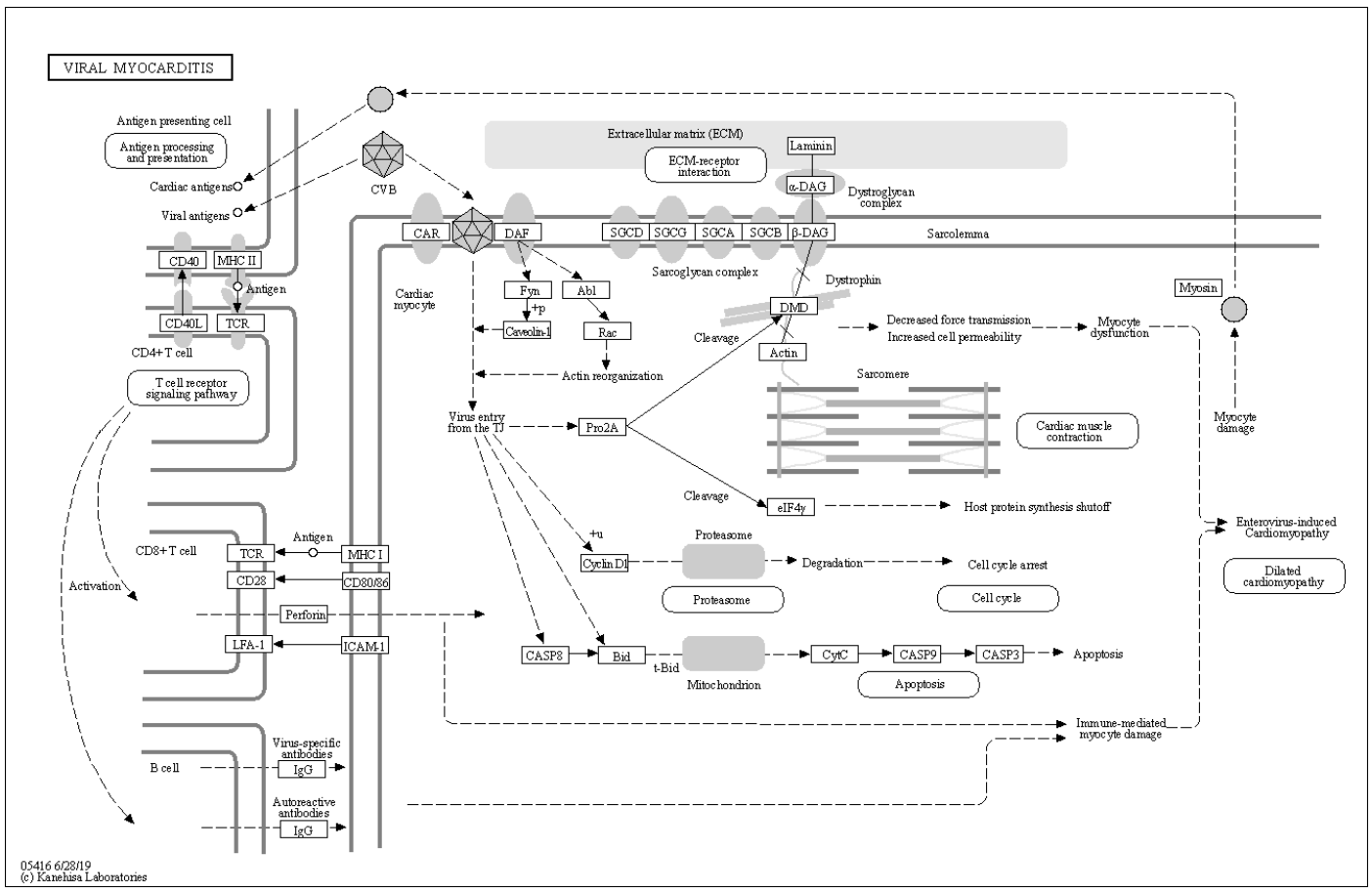

Kyoto Encyclopedia of Genes and Genomes (KEGG) analysis of metabolic pathways was conducted. The upregulation pathways of axon guidance (**A**), oocyte meiosis (**B**), regulation of actin cytoskeleton (**C**), and viral myocarditis (**D**) were found. Axon guidance pathways could regulate axon guidance, synaptogenesis, progenitor dynamics, and cell migration using a variety of mechanisms. Originally found to control local cytoskeletal rearrangements, axon guidance pathways might also regulate gene expression to control these complex developmental processes. In most mammals, oocytes were arrested at the diplotene stage, also called the Germinal Vesicle (GV) stage of the first meiotic prophase until a surge of gonadotrophin (particularly Luteinizing Hormone (LH)) from the pituitary stimulated the immature oocyte to resume the first meiosis and ovulate. Moreover, the actomyosin cytoskeleton generated force through the association with myosin motors and anchorage at subcellular structures, such as the plasma membrane. Key signaling pathways affected actin filament growth, bundling, branching, crosslinking, and severing. Besides, viral myocarditis was a rare cardiac disease associated with inflammation and injury of the myocardium. The downstream effects were a product of cooperation between viral processes and the innate immune response of host.

Appendix 8. KEGG (Kyoto Encyclopedia of Genes and Genomes) analysis of downregulation metabolic pathways.

A

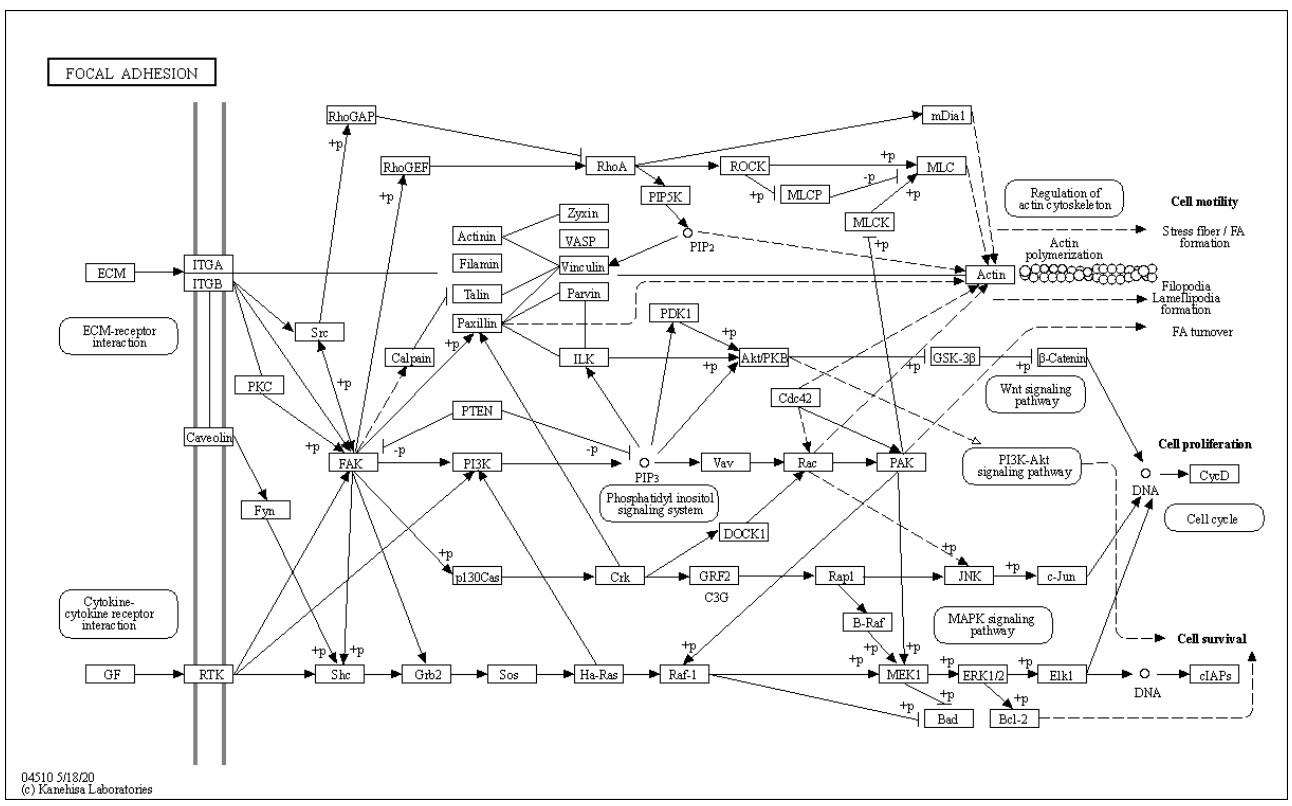

B

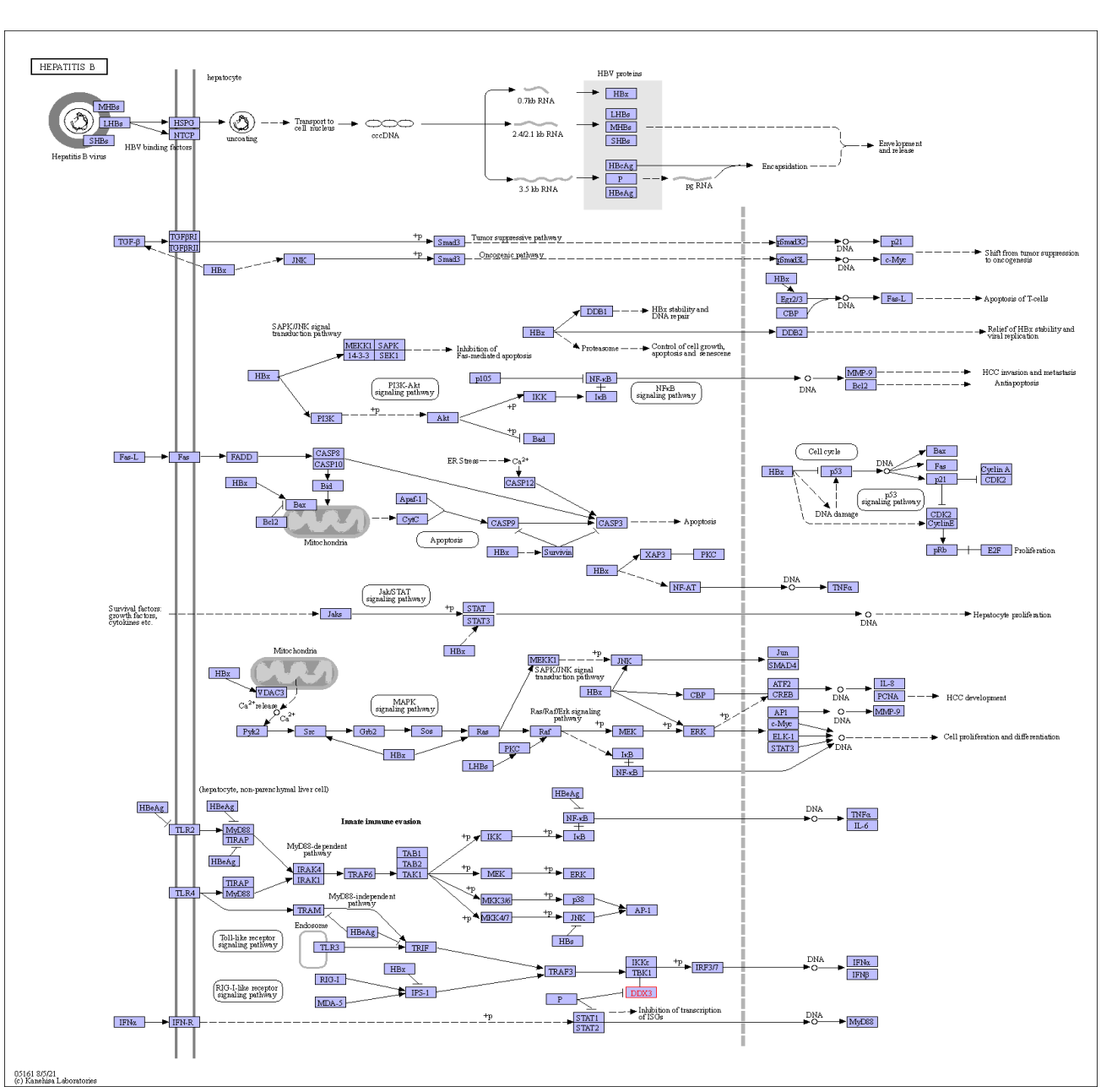

C

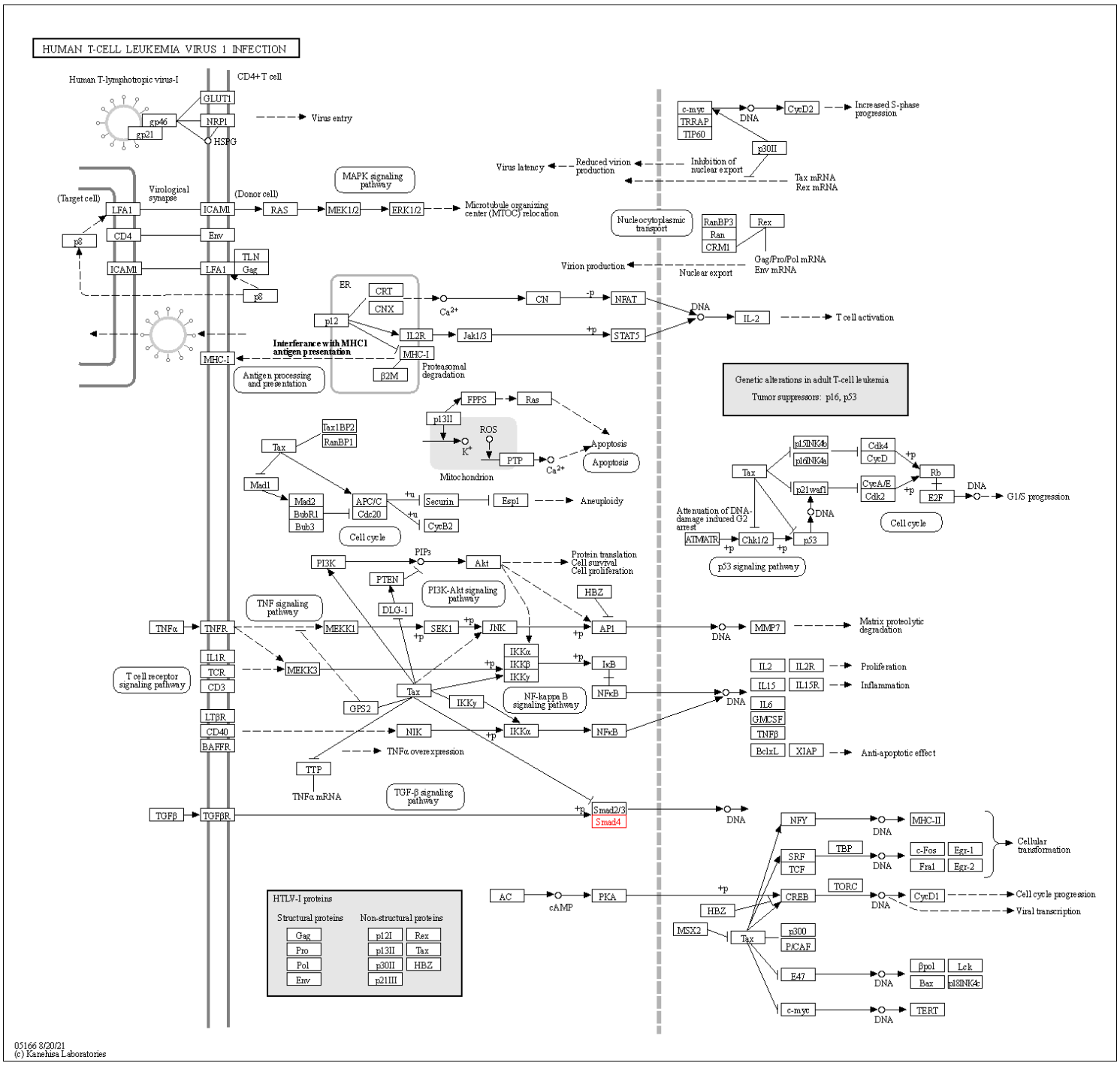
HUMAN T-CELL LEUKEMIA VIRUS 1 INFECTION
Human T-lymphotropic virus-I
CD4+T cell
GLUT1
gp46
NRP1
gp21
HSPG
Virus entry
(Target cell)
Virological synapse
(Donor cell)
LFA1
ICAM1
CD4
Env
p8
TLN
Gag
MAPK signaling pathway
RAS
MEK1/2
ERK1/2
Microtubule organizing center (MTOC) relocation
Interference with MHC1 antigen presentation
MHC-I
Antigen processing and presentation
ER
CRT
CNX
p12
β2M
Proteasomal degradation
Ca2+
CN
-p
NFAT
DNA
IL-2
T cell activation
IL2R
Jak1/3
+p
STAT5
c-myc
TRRAP
TIP60
CycD2
Increased S-phase progression
p30II
Virus latency
Reduced virion production
Inhibition of nuclear export
Tax mRNA
Rex mRNA
Nucleocytoplasmic transport
RanBP3
Ran
CRM1
Rex
Virion production
Nuclear export
Gag/Pro/Pol mRNA
Env mRNA
Genetic alterations in adult T-cell leukemia
Tumor suppressors: p16, p53
FPPS
Ras
p13II
ROS
K+
PTP
Ca2+
Apoptosis
Mitochondrion
Tax1BP2
RanBP1
Tax
Mad1
Mad2
BubR1
Bub3
APC/C
Cdc20
+u
Securin
Esp1
Aneuploidy
CycB2
Cell cycle
p15INK4b
p16INK4a
p21waf1
Cdk4
CycD
CycA/E
Cdk2
Rb
E2F
G1/S progression
Attenuation of DNA-damage induced G2 arrest
ATM/ATR
Chk1/2
p53
p53 signaling pathway
PI3K
PIPs
Akt
Protein translation
Cell survival
Cell proliferation
PTEN
PI3K-Akt signaling pathway
HBZ
TNF signaling pathway
DLG-1
TNFα
TNFR
MEKK1
SEK1
JNK
AP1
MMP7
Matrix proteolytic degradation
IL1R
TCR
CD3
T cell receptor signaling pathway
MEKK3
IKKα
IKKβ
IKKγ
IκB
NFκB
NF-kappa B signaling pathway
GPS2
IL2
IL2R
Proliferation
IL15
IL15R
Inflammation
IL6
GMCSF
TNFβ
BclxL
XIAP
Anti-apoptotic effect
LTβR
CD40
BAFFR
NIK
TNFα overexpression
TTP
TNFα mRNA
TGF-β signaling pathway
TGFβ
TGFβR
Smad2/3
Smad4
NFY
MHC-II
TBP
SRF
TCF
c-Fos
Fra1
Egr-1
Egr-2
Cellular transformation
TORC
AC
cAMP
PKA
CREB
CycD1
Cell cycle progression
Viral transcription
MSX2
p300
P/CAF
E47
βpol
Bax
Lck
p18INK4c
c-myc
TERT
HTLV-I proteins
Structural proteins
Gag
Pro
Pol
Env
Non-structural proteins
p12I
p13II
p30II
p21III
Rex
Tax
HBZ
05166 8/20/21
(c) Kanehisa Laboratories

D

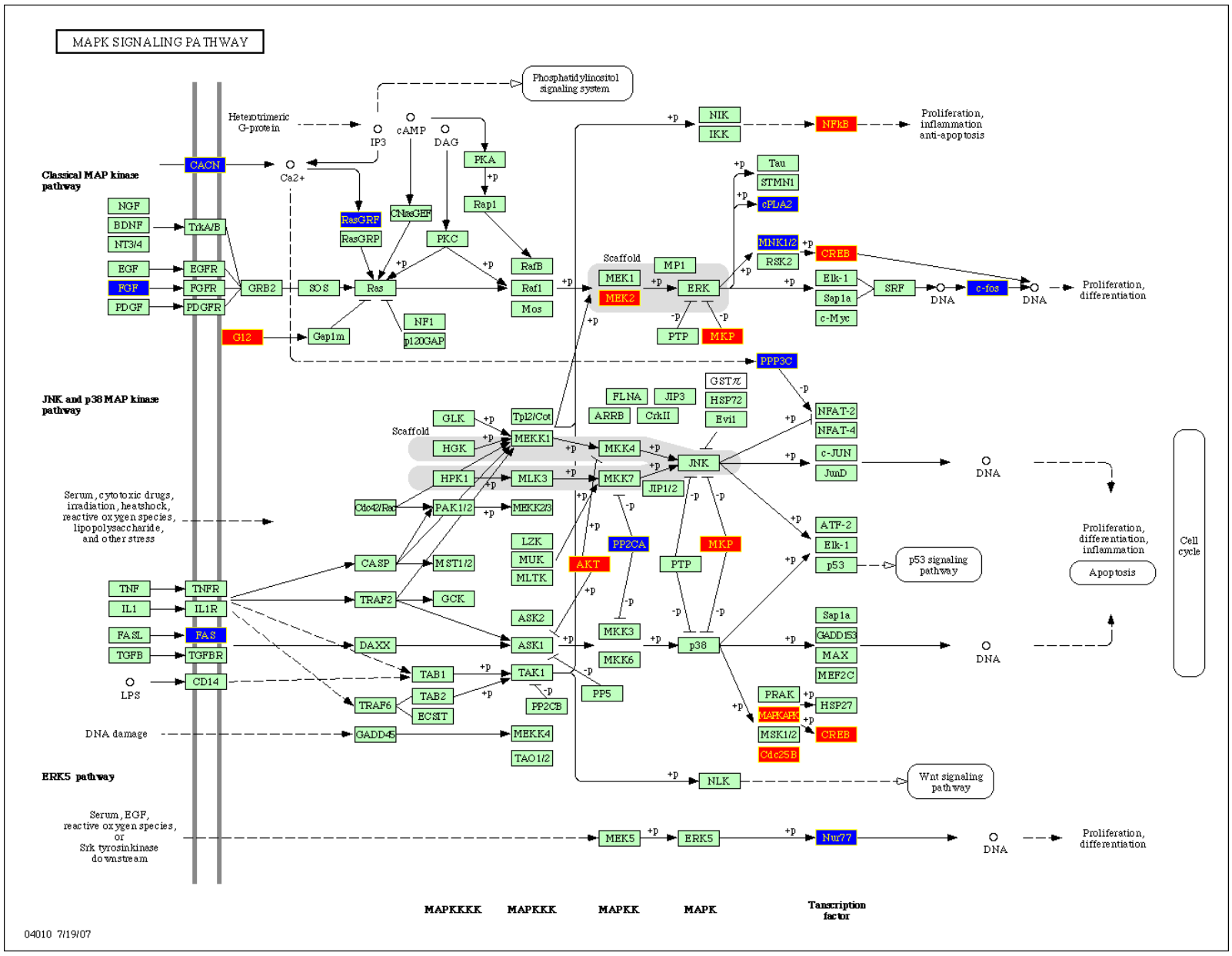
MAPK SIGNALING PATHWAY
Phosphatidylinositol signaling system
Heterotrimeric G-protein
cAMP
IP3
DAG
Ca2+
CACN
PKA
Rap1
RasGRF
CNrasGEF
RasGRP
PKC
Classical MAP kinase pathway
NGF
BDNF
NT3/4
EGF
FGF
PDGF
TrkA/B
EGFR
FGFR
PDGFR
GRB2
SOS
Ras
RafB
Raf1
Mos
G12
Gap1m
NF1
p120GAP
Scaffold
MP1
MEK1
MEK2
ERK
PTP
MKP
NIK
IKK
NFkB
Proliferation, inflammation anti-apoptosis
Tau
STMN1
cPLA2
MNK1/2
RSK2
CREB
Elk-1
Sap1a
c-Myc
SRF
c-fos
DNA
Proliferation, differentiation
PPP3C
JNK and p38 MAP kinase pathway
GLK
HGK
HPK1
Tpl2/Cot
MEKK1
MLK3
Scaffold
FLNA
JIP3
ARRB
CrkII
GSTπ
HSP72
Evi1
MKK4
MKK7
JNK
JIP1/2
NFAT-2
NFAT-4
c-JUN
JunD
Cdc42/Rac
PAK1/2
MEKK2/3
Serum, cytotoxic drugs, irradiation, heatshock, reactive oxygen species, lipopolysaccharide, and other stress
LZK
MUK
MLTK
CASP
MST1/2
AKT
PP2CA
MKP
PTP
ATF-2
Elk-1
p53
p53 signaling pathway
Proliferation, differentiation, inflammation
Apoptosis
Cell cycle
TNF
IL1
FASL
TGFB
LPS
TNFR
IL1R
FAS
TGFBR
CD14
TRAF2
GCK
ASK2
ASK1
DAXX
TAB1
TAB2
ECSIT
TAK1
TRAF6
PP2CB
PP5
MKK3
MKK6
p38
Sap1a
GADD153
MAX
MEF2C
PRAK
MAPKAPK
MSK1/2
HSP27
CREB
Cdc25B
DNA damage
GADD45
MEKK4
TAO1/2
ERK5 pathway
NLK
Wnt signaling pathway
Serum, EGF, reactive oxygen species, or Src tyrosinkinase downstream
MEK5
ERK5
Nur77
MAPKKKK
MAPKKK
MAPKK
MAPK
Transcription factor
04010 7/19/07

E

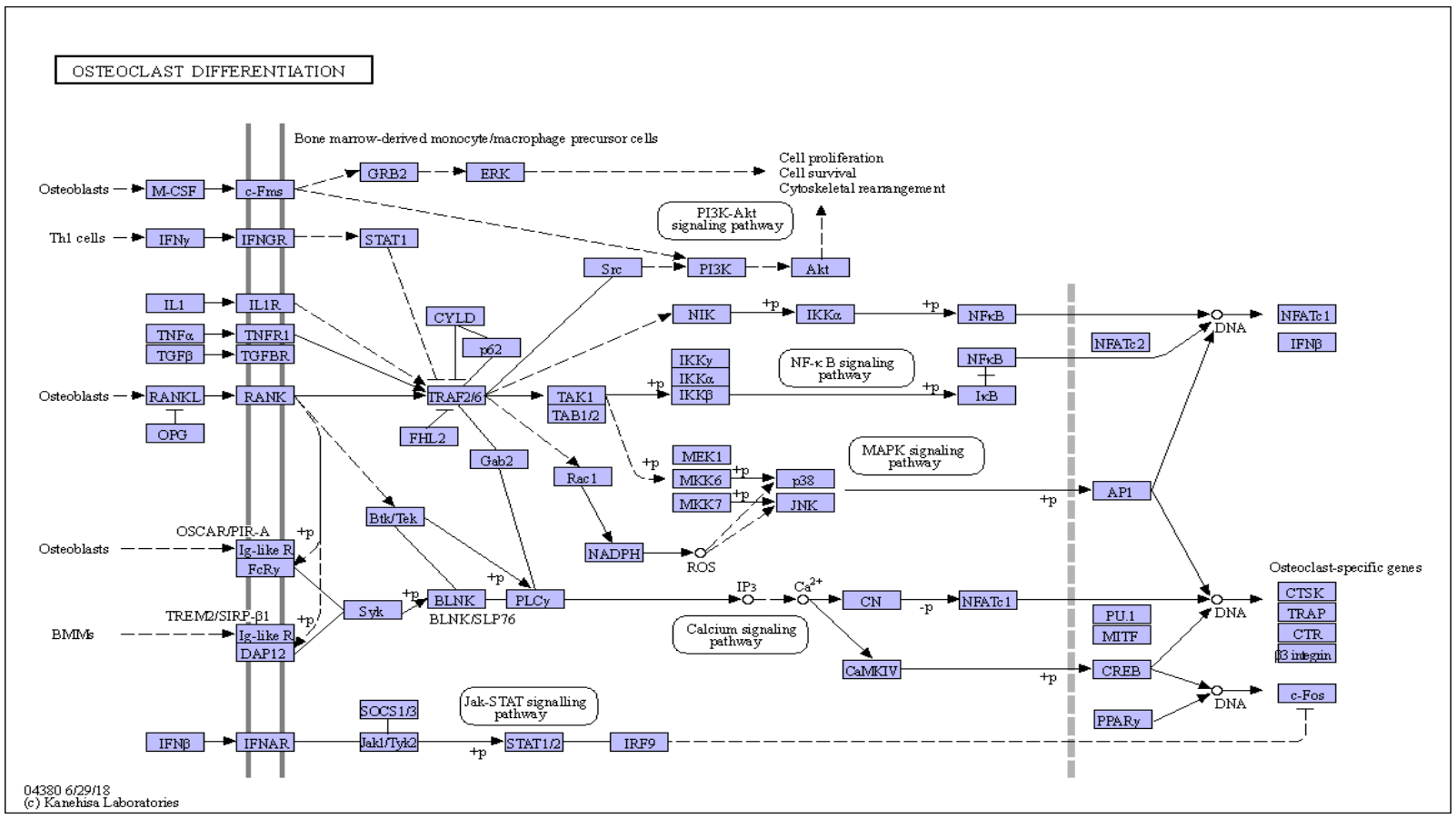
OSTEOCLAST DIFFERENTIATION
Bone marrow-derived monocyte/macrophage precursor cells
Osteoblasts
M-CSF
c-Fms
GRB2
ERK
Cell proliferation
Cell survival
Cytoskeletal rearrangement
PI3K-Akt signaling pathway
Src
PI3K
Akt
Th1 cells
IFNγ
IFNGR
STAT1
IL1
IL1R
TNFα
TNFR1
TGFβ
TGFBR
CYLD
p62
NIK
IKKα
NFκB
DNA
NFATc1
IFNβ
NFATc2
IKKγ
IKKα
IKKβ
NF-κB signaling pathway
NFκB
IκB
Osteoblasts
RANKL
RANK
OPG
TRAF2/6
FHL2
TAK1
TAB1/2
Gab2
Rac1
MEK1
MKK6
MKK7
p38
JNK
MAPK signaling pathway
AP1
Btk/Tek
OSCAR/PIR-A
Osteoblasts
Ig-like R
FcRγ
NADPH
ROS
Osteoclast-specific genes
CTSK
TRAP
CTR
β3 integrin
Syk
BLNK
PLCγ
BLNK/SLP76
IP3
Ca2+
CN
NFATc1
PU.1
MITF
TREM2/SIRP-β1
BMMs
Ig-like R
DAP12
Calcium signaling pathway
CaMKIV
CREB
c-Fos
PPARγ
SOCS1/3
Jak-STAT signalling pathway
IFNβ
IFNAR
Jak1/Tyk2
STAT1/2
IRF9
04380 6/29/18
(c) Kanehisa Laboratories

F

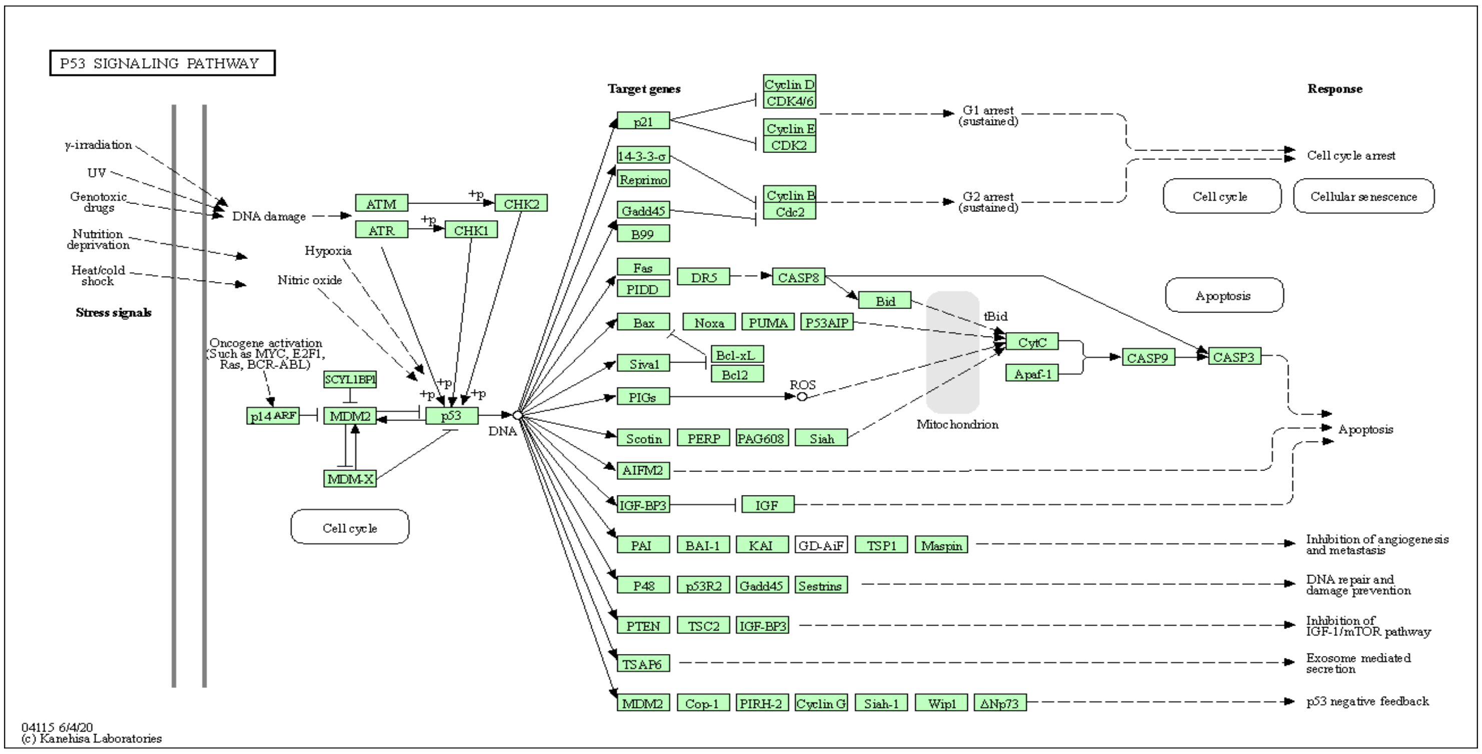

P53 SIGNALING PATHWAY
Target genes
Response
DNA damage
Stress signals
Cell cycle arrest
Apoptosis
04115 6/4/20
(c) Kanehisa Laboratories

G

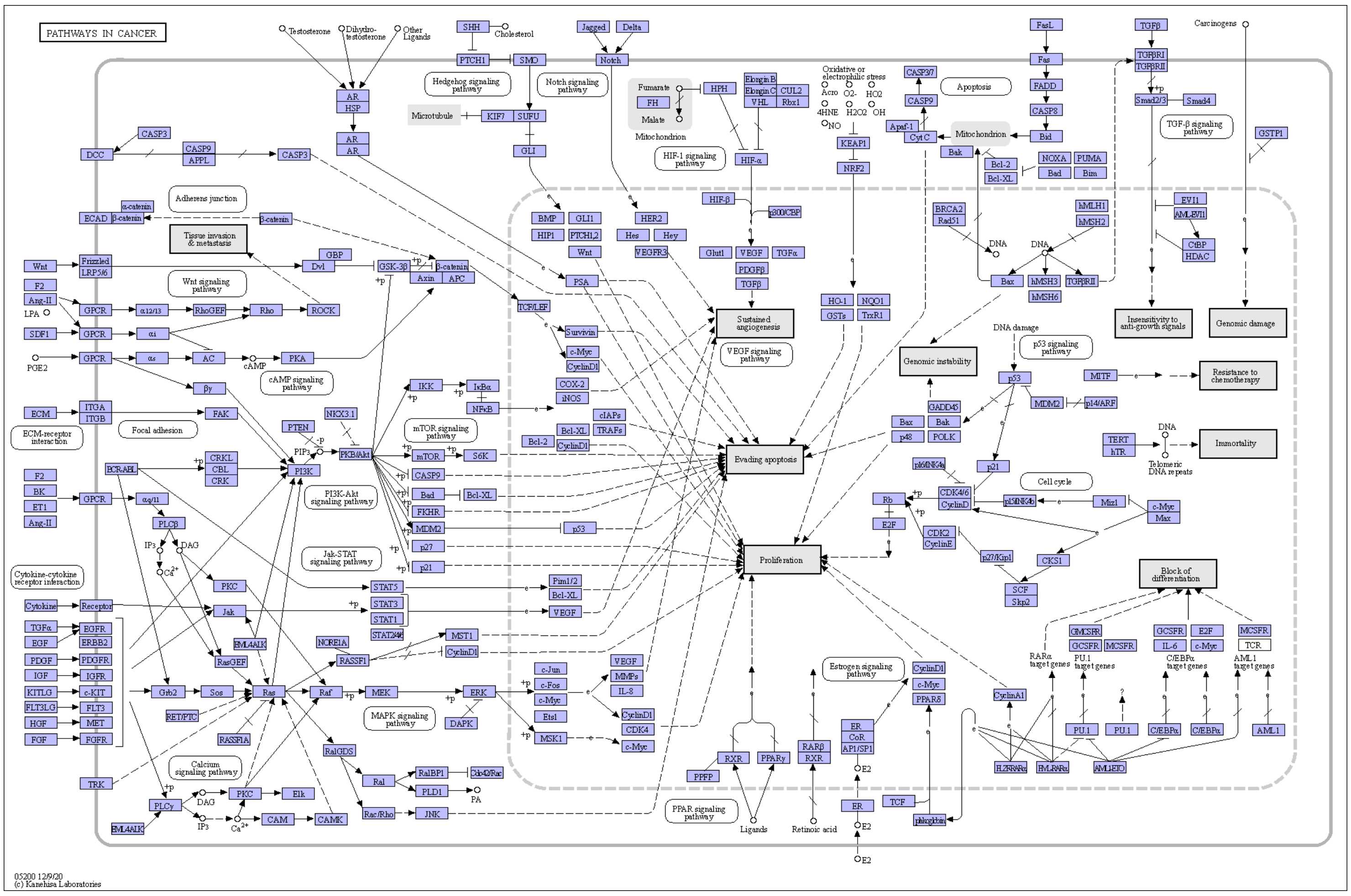

PATHWAYS IN CANCER
05200 12/9/20
(c) Kanehisa Laboratories

H

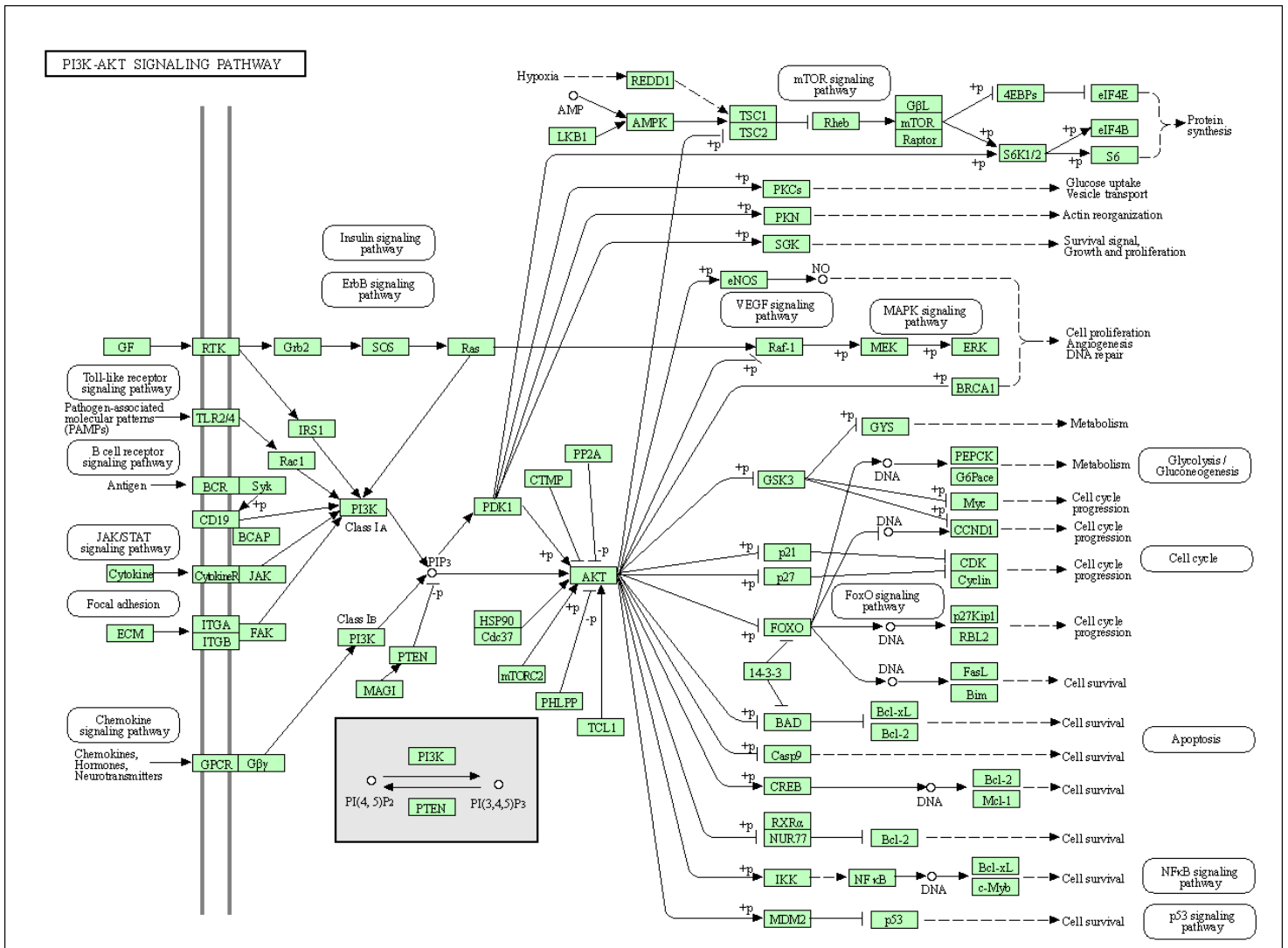

I

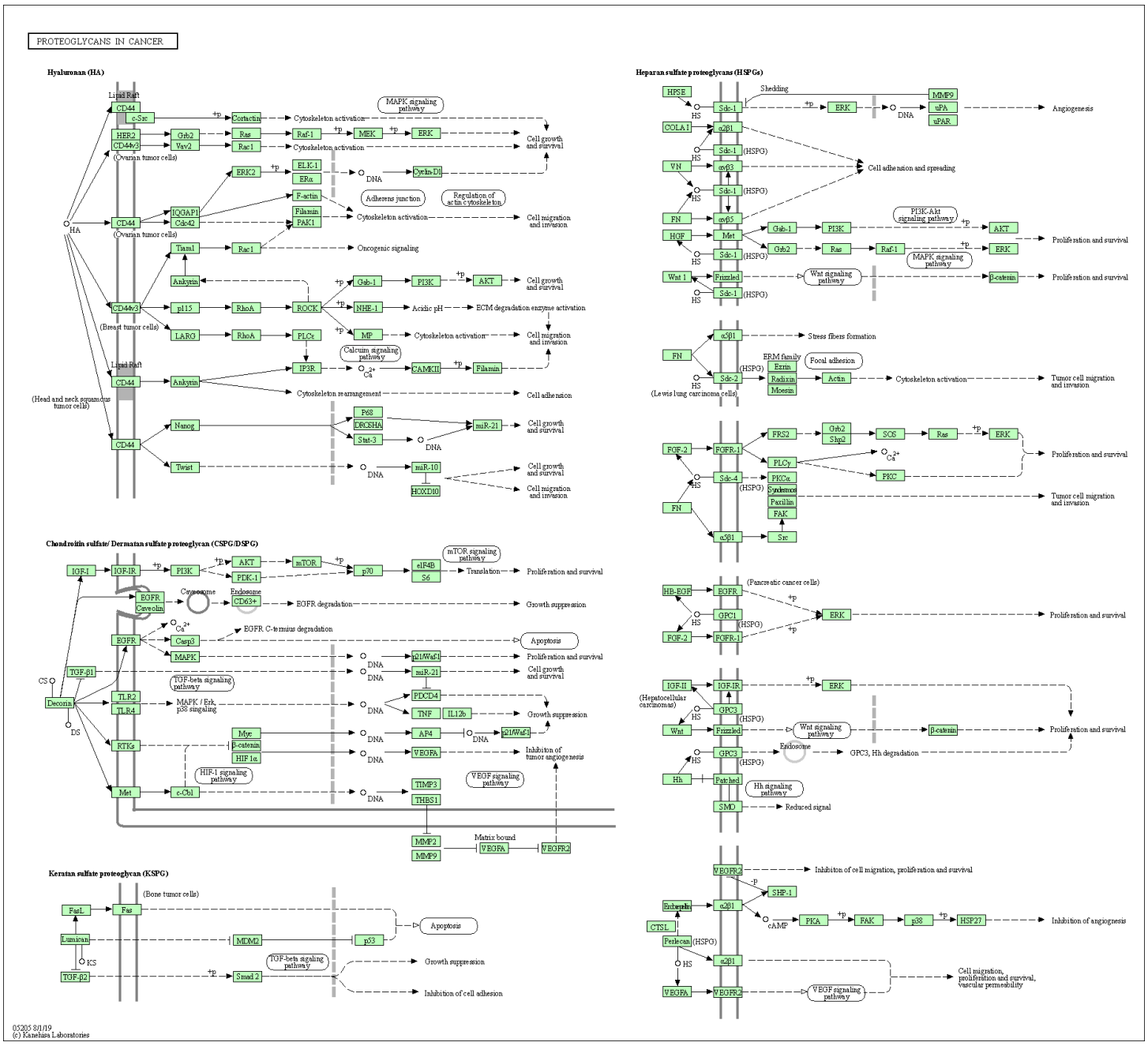
PROTEOGLYCANS IN CANCER
Hyaluronan (HA)
Heparan sulfate proteoglycans (HSPGs)
Chondroitin sulfate/ Dermatan sulfate proteoglycan (CSPG/DSPG)
Keratan sulfate proteoglycan (KSPG)
05205 8/1/19
(c) Kanehisa Laboratories

J

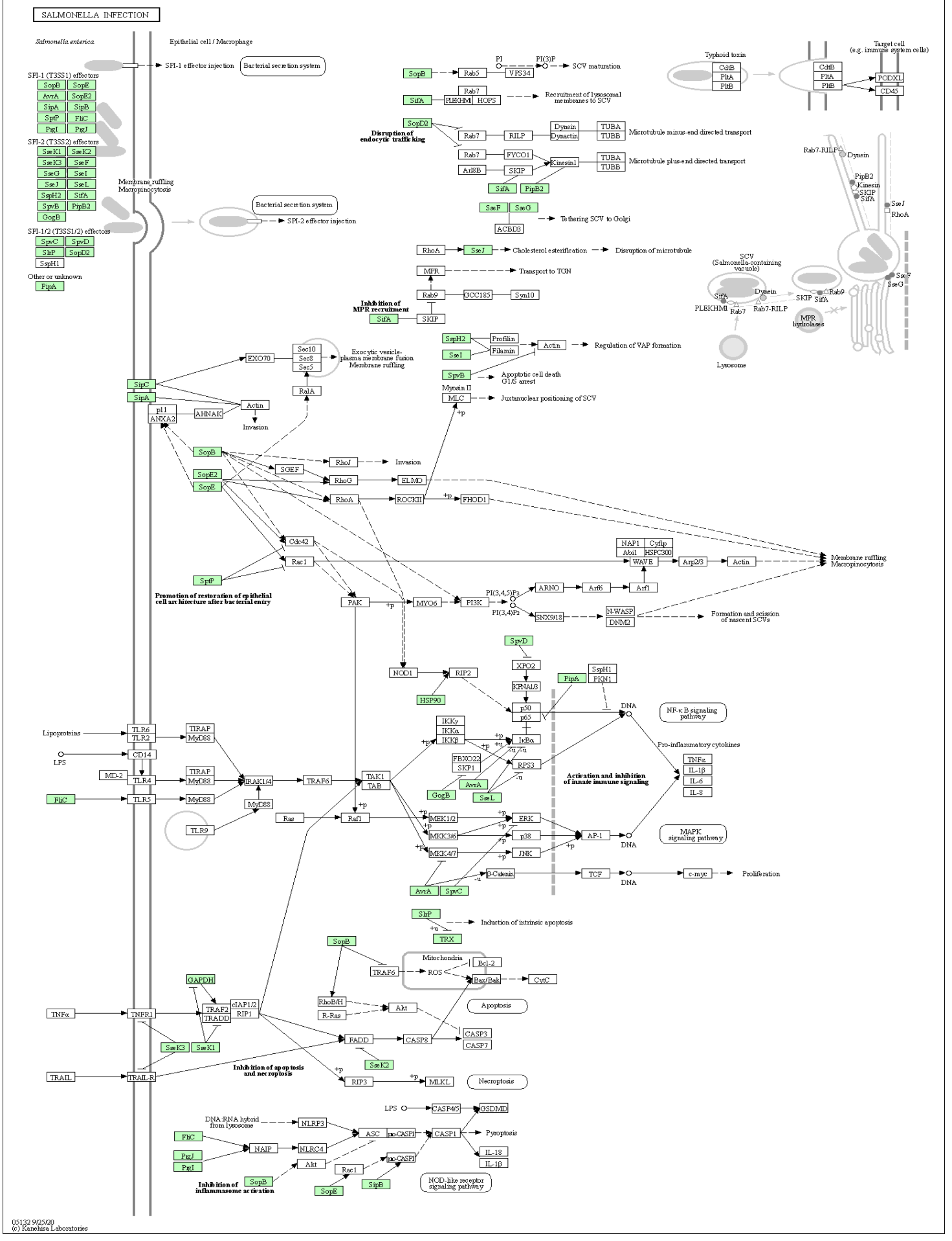

The downregulations of focal adhesion (**A**), hepatitis B (**B**), HTLV-1 infection (**C**), MAPK signaling pathway (**D**), osteoclast differentiation (**E**), p53 signaling pathway (**F**), pathways in cancer (**G**), PI3K-Akt signaling (**H**), proteoglycans in cancer (**I**), and salmonella infection (**J**) were obtained. Focal Adhesion Kinase (FAK) was a cytoplasmic tyrosine kinase that played critical roles in integrin-mediated signal transductions and also participated in signaling by other cell surface receptors. Additionally, HBV proteins targeted host proteins,

involved in a variety of functions, thus regulating transcription, cellular signaling cascades, proliferation, differentiation, and apoptosis. HTLV-1-infected cells presenting in breast milk (T cells, macrophages, and/or epithelial cells) could transmit the virus across the oral or gastrointestinal mucosa in several ways. The JNK and p38 MAPK signaling pathways were activated by various types of cellular stress. The JNK pathway consisted of JNK, a MAP2K such as MKK4 (SEK1) or MKK7, and a MAP3K such as ASK1, TAK1, MEKK1, or MLK3. In the p38 pathway, p38 was activated by MKK3 or MKK6, and these MAP2Ks were activated by the same MAP3Ks that function in the JNK pathway. The osteoclasts, multinucleated cells originating from the hematopoietic monocyte-macrophage lineage, were responsible for bone resorption. Osteoclastogenesis was mainly regulated by signaling pathways activated by RANK and immune receptors, whose ligands were expressed on the surface of osteoblasts. Signaling from RANK changed gene expression patterns through transcription factors like NFATc1 and characterized the active osteoclast. The P53-mediated cell signal transduction pathway played an important role in regulating the normal life activities of cells, and it was involved in the regulation of 160 genes. In addition, we knew of many situations where altered signaling pathways produced dramatic changes in cell survival, cell proliferation, morphology, angiogenesis, longevity, or other properties that characterized cancer cells. The PI3K-Akt and Ras-ERK pathways were just examples of oncogenic signaling pathways. Many of the genes commonly mutated in cancer encode the components or targets of PI3K-Akt and Ras-ERK pathways. Many proteoglycans (PGs) in the tumor microenvironment had been shown to be key macromolecules that contributed to the biology of various types of cancer including proliferation, adhesion, angiogenesis, and metastasis, affecting tumor progress. Salmonella infection usually presented as self-limiting gastroenteritis or the more severe typhoid fever and bacteremia. The common disease-causing Salmonella species in humans was a single species, *Salmonella enterica*, which had numerous serovars.

Appendix 9. Raw sequencing data statistics of microRNAs profiling.

	Blank 1	Blank 2	HCV R1	HCV R2
Total Reads	42,588,251	42,588,251	21,827,299	21,827,299
Length of Reads	101	101	101	101
Q20	42,352,349	34,623,530	21715735	20,504,479
Q20%	99.45%	81.30%	99.49%	93.94%
Q10	42,588,114	42,453,084	21,827,230	21,798,991
Q10%	100.00%	99.68%	100.00%	99.87%

Appendix 10. Quality of pretreatment microRNAs prolifing data.

Sample	Fastq	Clean	Mapp Genome	Mapp sRNA	Know miRNA	Novel miRNA
HCV	6,823,197	4,740,790	2,106,026	384,230	1,294	49,818
Blank	3,691,871	2,660,525	814,009	75,669	2,702	1,832

Appendix 11. The comparison for statistics results of clean reads of each database (Statics of RNA sequences from the individual libraries).

RNA type	Unique Read				Total Read			
	Blank	%	HCV	%	Blank	%	HCV	%
Total reads	1,701,271	100.00%	3,333,102	100.00%	3,691,871	100.00%	6,823,197	100.00%
Clean reads[a]	247,328	14.54%	685,639	20.57%	2,660,525	72.06%	4,740,790	69.48%
Matched genome[b]	126,293	51.06%	353,743	51.59%	814,009	30.60%	2,106,026	44.42%
bw-HCV[b]	3	0.00%	45	0.01%	5	0.00%	62	0.00%
Know-miRs[b]	17,001	6.87%	8,920	1.30%	109,831	4.13%	47,345	1.00%
rRNA[b]	17,985	7.27%	83,816	12.22%	62,669	2.36%	332,391	7.01%
tRNA[b]	1,344	0.54%	3,095	0.45%	1,919	0.07%	8,698	0.18%
snRNA[b]	1,719	0.70%	3,204	0.47%	4,882	0.18%	28,985	0.61%
snoRNA[b]	186	0.08%	188	0.03%	430	0.02%	470	0.01%
Rfam_other[b]	1,757	0.71%	5,222	0.76%	2,321	0.09%	10,358	0.22%
Repeat[b]	1,579	0.64%	1,630	0.24%	3,448	0.13%	3,328	0.07%
exon[b]	12,423	5.02%	41,197	6.01%	74,781	2.81%	128,383	2.71%
exon_antisense[b]	1,691	0.68%	5,327	0.78%	14,182	0.53%	35,755	0.75%
introns[b]	21,514	8.70%	53,794	7.85%	148,608	5.59%	456,253	9.62%
introns_antisense[b]	12,434	5.03%	35,160	5.13%	85,528	3.21%	253,351	5.34%
intergenic[b]	36,660	14.82%	112,190	16.36%	305,410	11.48%	800,709	16.89%
Un-annotated[b]	121,032	48.94%	331,851	48.40%	1,846,511	69.40%	2,634,702	55.58%

Note: [a], the percentage to the total reads; [b], the percentage to clean reads.